VIETNAM JOURNAL OF HYDROMETEOROLOGY

Research Article

Soil topography index and SCS – curve number approach in identifying hot spots of runoff potential areas

Anh Bui Khanh Van[1*]

[1] Faculty of Environmental Department – Ho Chi Minh City University of Natural Resources and Environment; bkvanh2020@gmail.com, bkvanh@hcmunre.edu.vn

*Corresponding author: bkvanh2020@gmail.com; bkvanh@hcmunre.edu.vn; Tel.: +84–908836115

Received: 05 May 2022; Accepted: 21 June 2022; Published: 25 June 2022

Abstract: Runoff reduction is the goal of soil and water conservation in agricultural watersheds. Through the runoff, many substances of soil such as sediment, nutrients have been eroded to end up in streams, rivers, and lakes. In decades, studies have revealed various mitigation, including structure and non–structure conservation ranging from field scale to watershed scale. However, the challenges for effectiveness improvement have increased in recent years within the impacts of anthropogenic activities such as land use land cover change and fluctuation in weather conditions. As a result, the runoff generation has been changing in both terms of quantitative and variable sources areas of runoff generation. From the understanding of runoff generation mechanisms, including infiltration excess and saturation excess, this study was conducted with the objective to propose an application of the Soil Topographic Index (STI) and the Soil Conservation Service Curve Number (SCS–CN) in identifying the areas with high runoff propensity. The method utilized GIS–based indices to indicate the high runoff potential areas. The ranking maps were evaluated by Wilcoxon rank sum test and Getis–Ord Gi* spatial statistics. Results demonstrated that there was a statistical significance of the greater STI in inundated cultivation than STI in cultivation areas. However, STI values were not statistically significant in pasture areas. Alternatively, the combination of STI and SCS–CN detected the statistical significance between calculated indices and inundated observed areas. In conclusion, the combination between STI and SCS–CN values is a potential method in redefining runoff generation hot spots.

Keywords: Runoff generation mechanism; SCS–Curve number; Soil topographic index; Ranking approaches; Hot spots and cold spots.

1. Introduction

Runoff and agricultural best management practices (Agricultural BMPs) in soil and water conservation has been a research topic for decades. In 1979, agricultural BMPs controlling runoff resulted in effectiveness of agricultural BMPs was pointed out [1]. Accordingly, the appropriate agricultural BMPs is the lining up between types and purposes of BMPs, which is relevant to the term of targeted conservation, recently. For this reason, the misleading in runoff generation which may cause inaccuracy in identifying high runoff areas has been mentioned in some researches. Since then, many of researches with the purposes to fill the deficiency between BMPs design and the runoff generation mechanisms have been conducted [2–3]. Most recently, 7Rs – Right product, right conservation practices, right

place, right scale, right rate, right method, and right time – again plays an important role in precision of soil and water conservation [4].

Subsequently, there has been many studies concerning either differentiation or combination between infiltration excess and/or saturation excess in runoff generation mechanisms, which influence the results of runoff generation in term of temporal scales and variable sources areas of runoff proneness [2, 5–10]. Importantly, the implication that the Soil Conservation Service Curve Number approach (SCS–CN method) should not be applied in the manner of only infiltration excess and excluding of saturation excess amongst many debates about the application of SCS–CN in rainfall–runoff model [8, 11].

Therefore, in this study, quantitative indices inferring qualitative rank of runoff generation were proposed with the approach of hot spots emergence mechanisms. Hot spot definition was initially proposed in 2003 [12]. The concept of hot spots are areas that show disproportionately high reaction rates related to the surrounding area (or matrix). Hot moments are short periods of time that show disproportionately high rates relative to longer intervention time periods. Emergence of hot spot hot moments highlighted the heterogeneity characteristics of the phenomenon. Hot spot means the spatial intensive concentration of phenomenon at high rate, and hot moment refers to the temporal dimension, during periods of time the phenomenon was enhanced. Hot spots and hot moments may overlap or separate. Most importantly, hot spots identification strongly depends on generating mechanisms. In other word, the meaning of understanding the mechanism is that it can be utilized to predict hot spots in the future [12].

In this research, runoff occurrence was considered a hot spot–hot moment approach due to similarity in disproportionately insightful emerged mechanism. Therefore, utilizing the hot spots emergence mechanism to contribute the research methodology is a potential approach. Also, hot spot theory can apply to emerge the hot spots of critical source areas of sediment, nitrogen and phosphorus. The second condition is the spatial scale and temporal scale which are the considerable factors in hot spots identification. For instance, the forming of surface runoff depends on the integrated impacts of topology, rainfall, soil profile and crop–scape in agricultural watersheds. The high runoff propensity area is the area that satisfies all the high conditions of four features. Therefore, the ultimate distribution of high runoff areas is defined as the areas within the overlapping of these characteristics.

GIS – based indices application has not been a new approach but there is still a lack of using GIS – based indices to propose the hot spots of runoff generation mechanisms in combination of SCS – Curve number approach and the Soil Topographic Index (STI). From the perspective of runoff generation mechanisms, including infiltration excess and saturation excess, this study is conducted with the objective to propose an application of GIS – based indices in identifying the areas with high runoff tendency. The study focuses on answering the question of how to precisely define the high runoff areas in order to propose a suitable soil and water conservation practices and explicit placement of agricultural BMPs. In order to answer the research question, the analogy of combination SCS–CN and STI was proposed.

2. Methodology

Study area was Callahan Creek watershed in Boone County in Missouri with the area approximately 21,960 acres (89 km^2). Location of the basin was as in figure 1. The land use land cover (LULC) types mainly comprise forestry and agricultural areas such as corn, soybean, winter wheat, hay, grass, pasture, and deciduous forest. Also, this area is one of PL–566 watershed projects – The Watershed Protection and Flood Prevention Act.

The Digital Elevation Model (DEM) was downloaded from the U.S. Geological Survey (USGS) database and soil survey data, land use land cover from the U.S. Department of Agriculture (USDA) cropland database at 30m × 30m resolution. The record of inundated areas for Missouri and Illinois in May and June 2019 from National Agricultural Statistic

Services (USDA–NASS) was employed as observed data. The observed inundated cultivation and inundated pasture in this area was extracted; afterward, this observed data was converted to point vector data by GIS toolboxes in order to analyze attribute data and execute statistical hypotheses test by R packages.

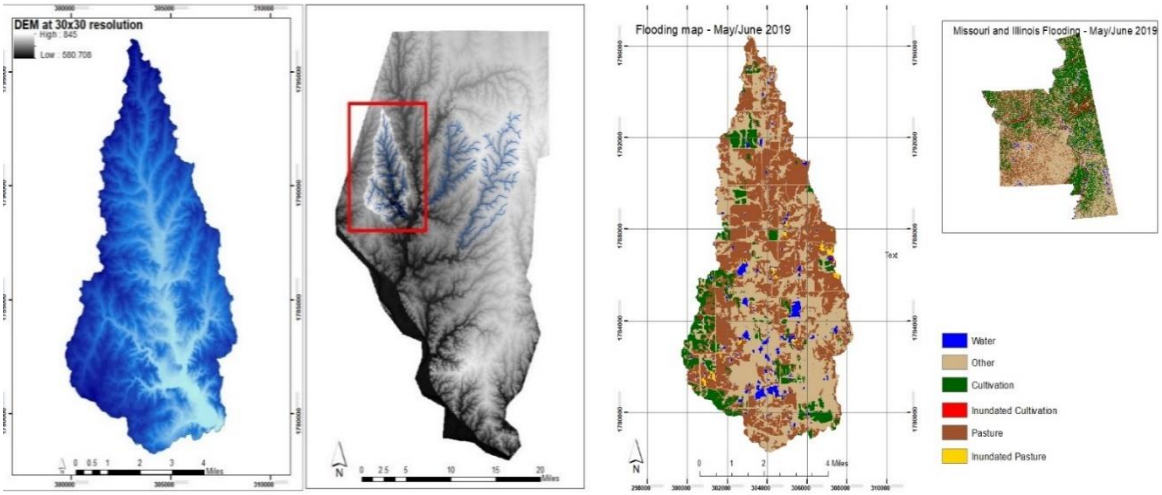

Figure 1. Location of Callahan basin (on the left) and inundated map of Callahan basin (on the right), Boone County, Missouri.

In this study, a proposed approach is that the curve number method can contribute to qualitative evaluation in the linkage of hydrologic soil groups, land–use types, and the condition of land cover. SCS–CN method was applied by the U.S. Department of Agriculture (USDA) in 1972, SCS–CN values indicate the linkage of soil types, antecedent moisture condition, land use types, and surface conditions [13]. Employing SCS–CN to produce runoff map was mentioned in previous study [14]. Subsequently, the STI was originally developed based on the Topographic Wetness Index (TWI) which was respectively published in 1979, 2000 and 2002 [9, 10, 15]. This index demonstrated interaction between topography and soil physical features such as depth of soil and saturated hydraulic conductivity. Applying TWI to produce runoff ranking map was proposed in studies [3] and other indexes for targeted agricultural BMPs was also mentioned [16]. Most significant, the Soil Topographic index (STI) was explained and applied in previous studies [9, 17, 18]. According to, STI was calculated as in formulation (1):

$$\mathrm{STI} = \ln\left(\frac{\alpha_i}{\tan(\beta_i)k_s D}\right) \quad (1)$$

where STI is soil topography index; α_i is upslope contributing area per unit contour length (m); $\tan(\beta_i)$ is the local surface topographic slope; k_s is the mean saturated hydraulic conductivity of the soil (m/day); and D is the soil depth to restrictive layer (m).

After that, the calculated raster data was executed spatial join with the SCS–CN and converted to point vector data, employing the explanation and the guidelines from USDA in 1986 to identify suitable curve number values [13]. Accordingly, there are four different types of SCS–CN values depending on Hydrologic Soil Group (HSGs) in drained conditions and LULC conditions. The first letter in the dual HSGs applies to the drained condition, the second letter in the dual HSG applies to the undrained condition. As a result, there were four different scenarios of SCS–CN values according to the combination of draining conditions and LULC conditions. However, the study compared the observed inundated maps at the time in which the extreme inundated event occurred in May of 2019. Therefore, the others

scenarios were eliminated, only SCS–CN values of undrained condition and LULC in poor condition were taken into evaluation.

Notably, there were inconsistency between LULC map and observed inundated map. There were 25 LULC types, while only 6 reclassified types of inundated areas were in the inundated areas map. For example, the deciduous forest in LULC data were reclassified into 6 different types in inundated map which were inundated cultivation, cultivation, inundated pasture, pasture, other, and water areas. Beside the uncertainty of LULC and flooding map, the assumption which were HSGs, LULC, saturated hydraulic conductivity, depth to restrictive layer of the soil in mean values and depth to restrictive layer as in the soil survey database were assigned to calculate STI indices and determine SCS–CN values. Ideally, these parameters should be as realistic as possible to reduce uncertainty in calibration.

In spatial statistic, three distinctions of ranking approaches were proposed and assessed by Getis–Ord Gi* hotspots z scores developed by Getis and Ord to analyze spatial patterns [19–21]. Spatial autocorrelation was developed based on the first law of geography which is "everything is related to everything else, but near things are more related than distant things" [22]. Getis–Ord Gi* scores were calculated to illustrate the spatial autocorrelation, though this statistic cannot interpret the reason why locations that have statistically significant hot spots or cold spots. In other words, this method cannot identify the mechanism which causes hot spots or cold spots. In this study, this approach was utilized to clarify the number and the location of hot spots. Above all, hot spots of three distinct ranking approaches infer the three STI and SCS–CN combinations. Finally, the three distinguished distributions of calculated hot spots were compared with the distribution of observed inundated data.

3. Results and Discussions

Subsequently, the STI index of Callahan Creek ranged from 3.4 to 27.5 (Figure 2). The interpretation is that the higher STI and SCS–CN values represent the higher runoff potential. STI distribution was highly skewed to the right which is not normal distribution with the density curve is not symmetric and bell–shaped. Quantile plot of SCS–CN values describing poor and undrained condition in inundated areas and other types in flooding map evidenced a non–normal distribution. The plots indicated the systematic deviations from a straight line. Outliers appeared as points that were far away from the overall pattern of the plot. Therefore, the statistical method of non–parametric approach was appropriate in these conditions.

The attribute data obtained two types of variables, including numerical variables and categories variables. SCS–CN and STI are numerical variables. The inundated areas of flooding map such as cultivation and pasture are categories variables. According to the quantile plot of the variables, variable distributions are not normal distributions. Therefore, the non–parametric test which are Kruskal Wallis rank sum test, Wilcoxon rank sum test, bootstrapping interval confidence calculation were applied to compare between inundated areas and out of inundated areas. Spatial point data using Getis – Ord Gi* hot spot was applied to identify significant hot spots. The principles of combination between SCS–CN and STI were summarized as in figure 3.

In this proposed method, observation data of inundated areas was important since it was utilized to assess the accuracy of the proposed indices. In observed data, each pixel represented the condition of inundated areas. In this study area, the inundated map recorded the historical inundated of Missouri in May 2019. Accordingly, the inundated areas mainly distributed in the cultivated areas and pasture areas. This distribution not only occurred in nearly streamflow location. The higher SCS–CN and STI inferred the higher potential of runoff. In this study, the condition of LULC at the recorded extreme event was dramatically poor condition without cover crops and low capacity of drainage condition.

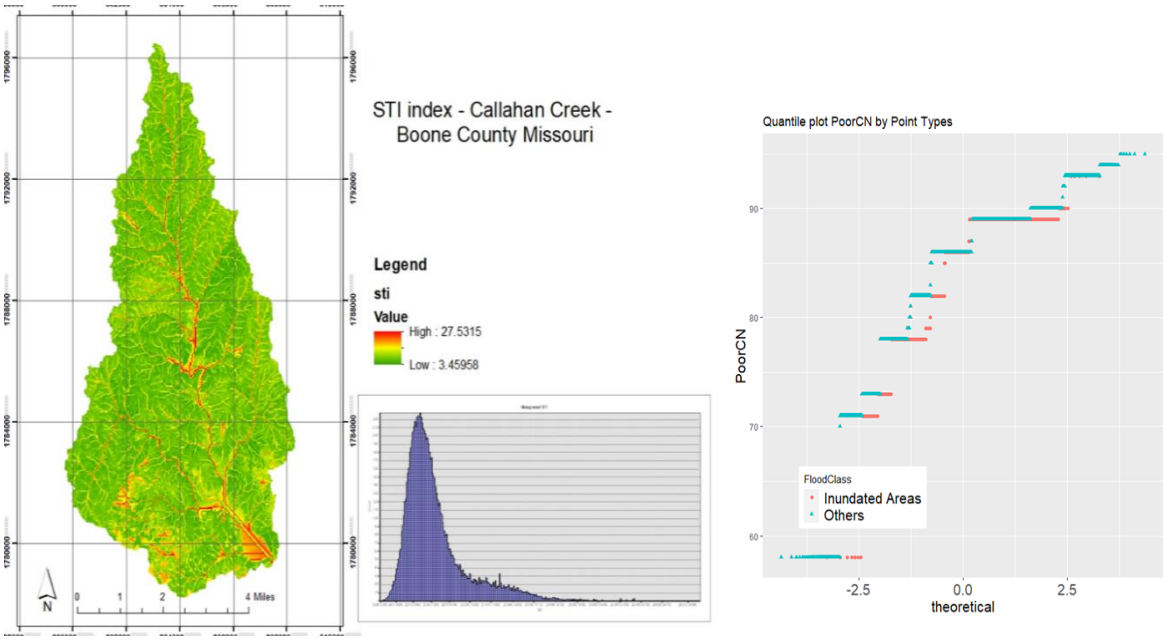

Figure 2. Narrative description of STI and SCS–CN values in poor and undrained conditions.

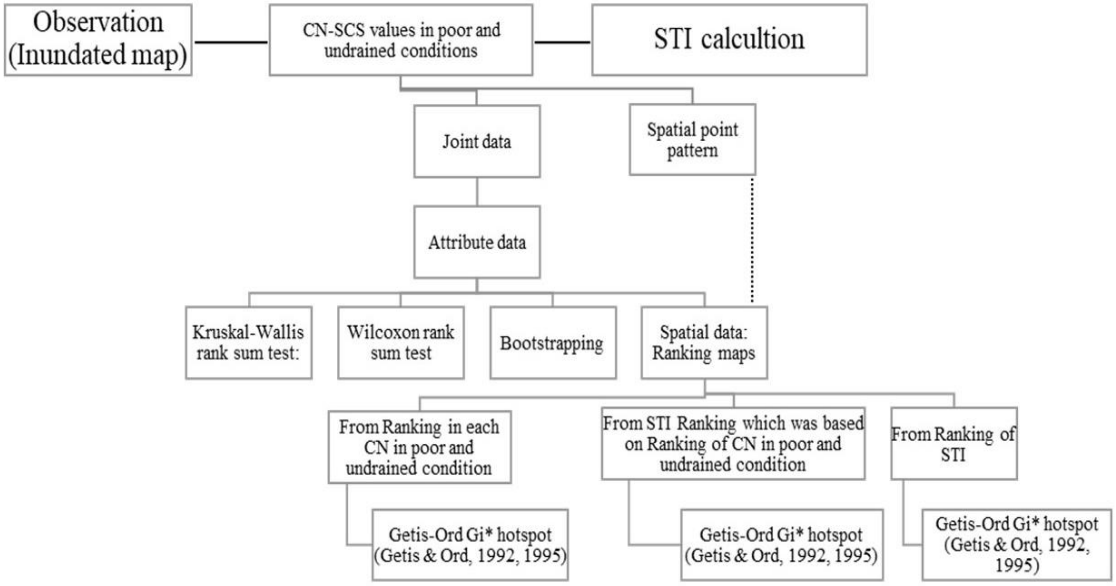

Figure 3. The proposed method of combination between SCS–CN and STI.

Comparing median values between STI inundated areas and STI out of inundated areas illustrated that there was a significant difference between STI and SCS–CN in poor and undrained condition of all groups. The Null hypothesis was that median of STI in inundated areas and median out of inundated areas were equal. The alternative hypothesis was that median in inundated areas was different from median out of inundated areas. Figure 4a revealed that p value proved statistically significant difference in pair comparisons of STI between inundated cultivation and cultivation, inundated pasture and inundated cultivation, cultivation and pasture. However, STI between inundated pasture and pasture were not different. Figure 4b revealed that p value indicated statistically significant difference in pair comparisons of all SCS–CN in poor and undrained condition, but SCS–CN in inundated areas were less than those of drained areas. Figure 4c, density distribution highlighted the higher values of STI in inundated cultivation in comparison to STI in cultivation. In contrast, figure 4d revealed the lower values of SCS–CN in inundated cultivation.

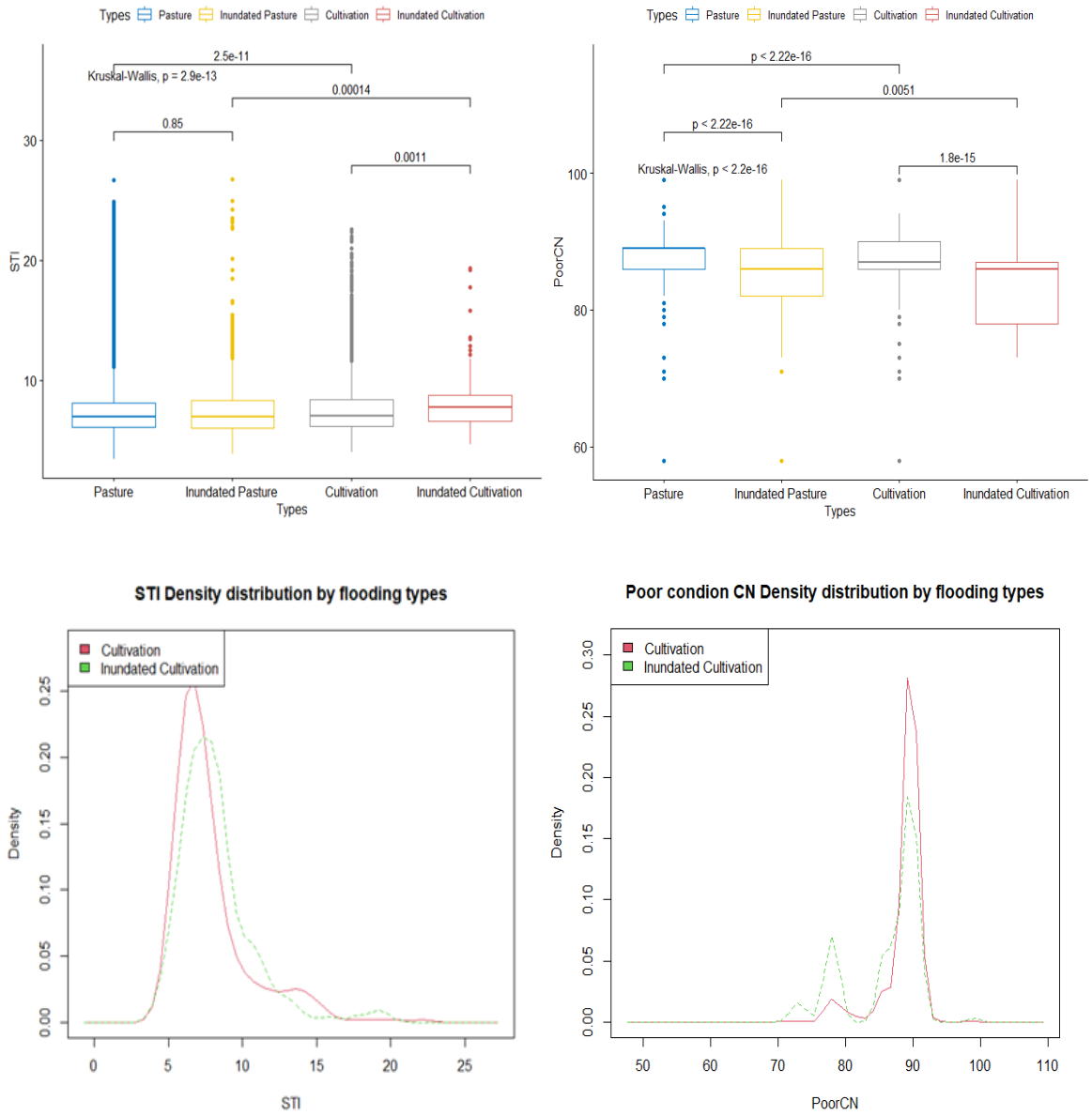

Figure 4. Kruskal–Wallis rank sum test: (a) Kruskal–Wallis test of STI in 4 types of flooding maps; (b) Kruskal–Wallis test of SCS–CN in poor and undrained condition in 4 types of flooding maps; (c) Density distribution of STI in cultivation and inundated cultivation; (d) Density distribution of SCS–CN in cultivation and inundated cultivation.

Table 1. Wilcoxon rank sum test in pair comparison.

Wilcoxon rank sum test in the undrained condition					
Variables	Group x	Group y	W	p–value	Alternative Hypothesis
STI	Inundated_Cultivation	Cultivation	721189	0.0005622	Greater
PoorCN	Inundated_Cultivation	Cultivation	375646	9.25E–16	Less
PoorCN	Inundated_Pasture	Pasture	19321152	2.20E–16	Less

In order to evaluate in pair comparison, Wilcoxon rank sum test computed the value of p as in Table 1. In STI comparison between inundated cultivation and cultivation, p value was 0.0005622, the null hypotheses were rejected and the alternative hypotheses that medians of STI distributions for inundated cultivation were statistically significant and greater than

that of cultivation areas. It means that the STI distributions for inundated cultivation are likely shifted to the right of the STI distributions for cultivation. In SCS–CN evaluation, p values are < 2.2e–16, the null hypotheses were rejected and the alternative hypotheses that medians of SCS–CN values distributions for inundated cultivation were statistically significant and less than those of cultivation and pasture. It means that the SCS–CN values distributions for inundated cultivation and inundated pasture are likely shifted to the left of the SCS–CN distributions for cultivation and pasture. It infers that SCS–CN values in all cases of inundated areas were less than those of drained areas.

Bootstrap confidence interval calculations in table 2 emphasized the similarity to Wilcoxon rank sum test. Only confidence interval of STI between inundated cultivation and cultivation were less than 0, bootstrap confidence interval based on 10,000 bootstrap replicate times were –0.73851. The others results were greater than or equal to 0. These results reinforced the hypothesis that STI in inundated cultivation were higher than STI values in cultivation areas.

Table 2. Bootstrap confidence interval based on 10000 bootstrap replicates.

Variables	Group 1	Group 2	Resample	Original	BootBias	BootSE	Method	BootMed
STI	Inundated_Cultivation	Cultivation	10000	–0.73623	0.003979	0.21386	Med diff	–0.73851
STI	Inundated_Pasture	Pasture	10000	0.0188	0.002326	0.063783	Med diff	0.01735
PoorCN	Inundated_Cultivation	Cultivation	10000	1	0.0524	0.38369	Med diff	1
PoorCN	Inundated_Pasture	Pasture	10000	0	0.56395	1.1	Med diff	0

The previous results clarified that separately applied STI and SCS–CN values insufficiently reflected the complex mechanisms of runoff generation in a basin. It is crucial to appropriately assemble indices to expose the underlying dynamic processes. Thus, STI and SCS–CN in poor and undrained condition were unified to highlight the trend. In figure 5, the boxplot comparison of STI and SCS–CN in poor condition between inundated cultivation and cultivation in undrained condition indicated that the p value of Wilcoxon rank sum test at SCS–CN 90 was significant. For the inundated pasture, p values of Wilcoxon rank sum test at SCS–CN 78 and 79 were significant. At SCS–CN 71, 82, 86, STI of pasture were higher than STI of inundated pasture.

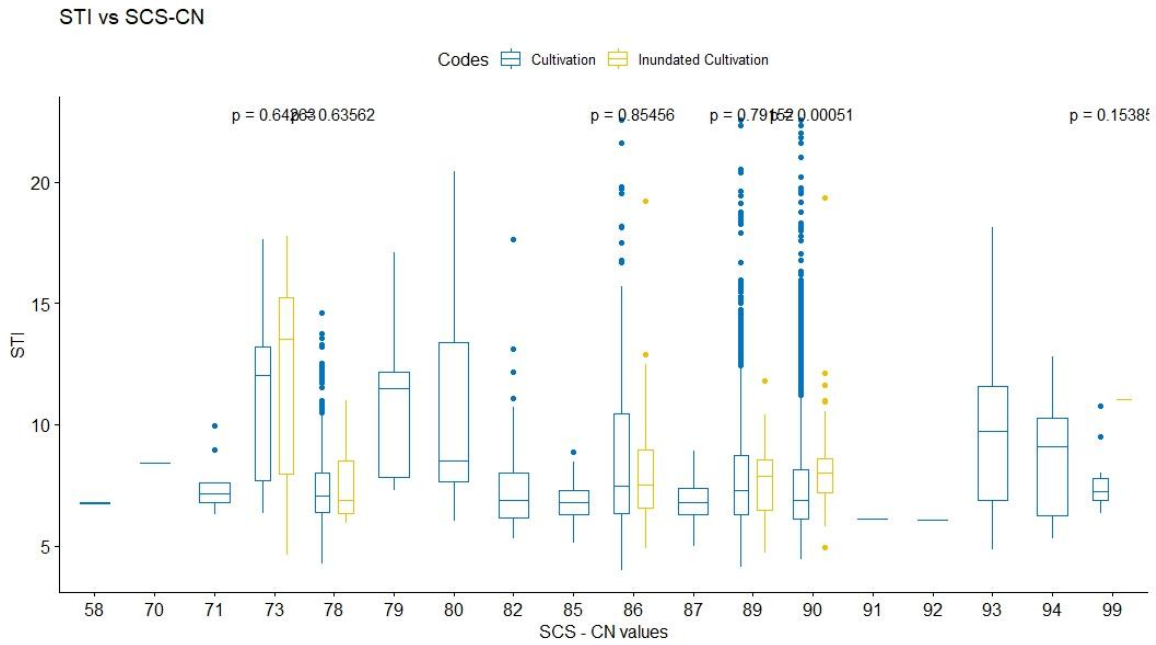

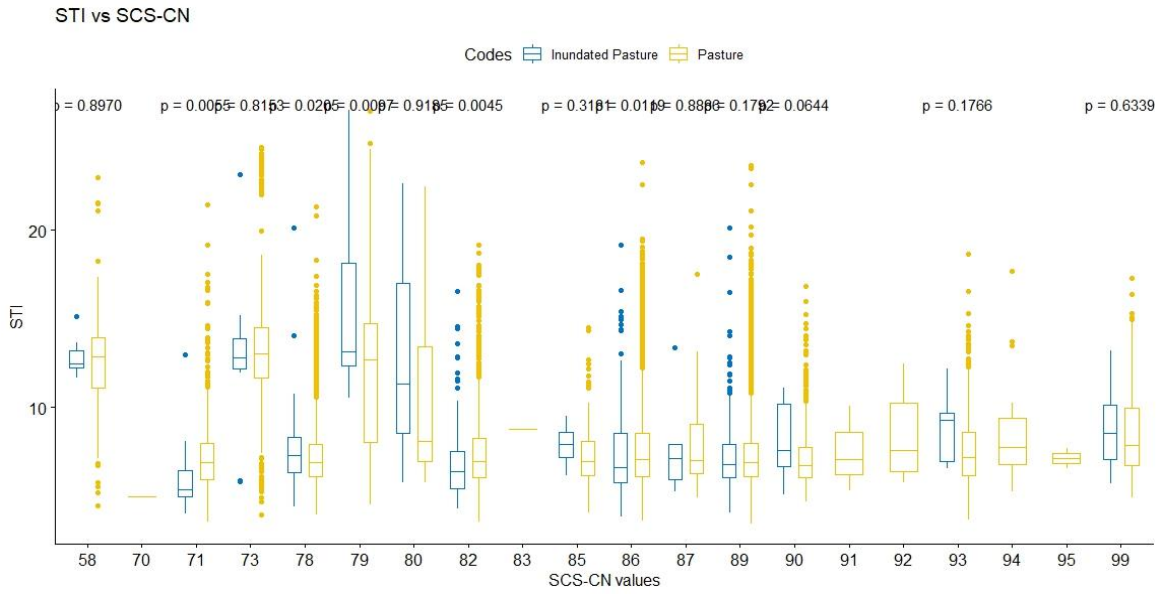

Figure 5. Parallel comparison of STI and SCS–CN in poor and undrained condition; (a) Wilcoxon rank sum test of STI in pairs inundated cultivation and cultivation in each SCS–CN value; (b) Wilcoxon rank sum test of STI in pairs inundated pasture and pasture in each SCS–CN value.

According to the validated results, there were three different ranking approaches. The first ranking was solely based on STI values, the second approach was from STI ranking which was based on the rank of SCS–CN in poor and undrained condition, the third approach was from the ranking in each SCS–CN in poor and undrained condition. Subsequently, Getis–Ord Gi* hotspots were calculated in each ranking map utilizing GIS toolboxes. In the first approach (Figure 6), correlation coefficient between STI and STI ranking was 1 because the ranking was only based on STI values. This ranking simplified that a point with a larger STI represented a higher STI ranking. Overall, the STI ranking changed exponentially with the STI values from SCS–CN 58 to SCS–CN 99. Curve number values did not affect this type of ranking.

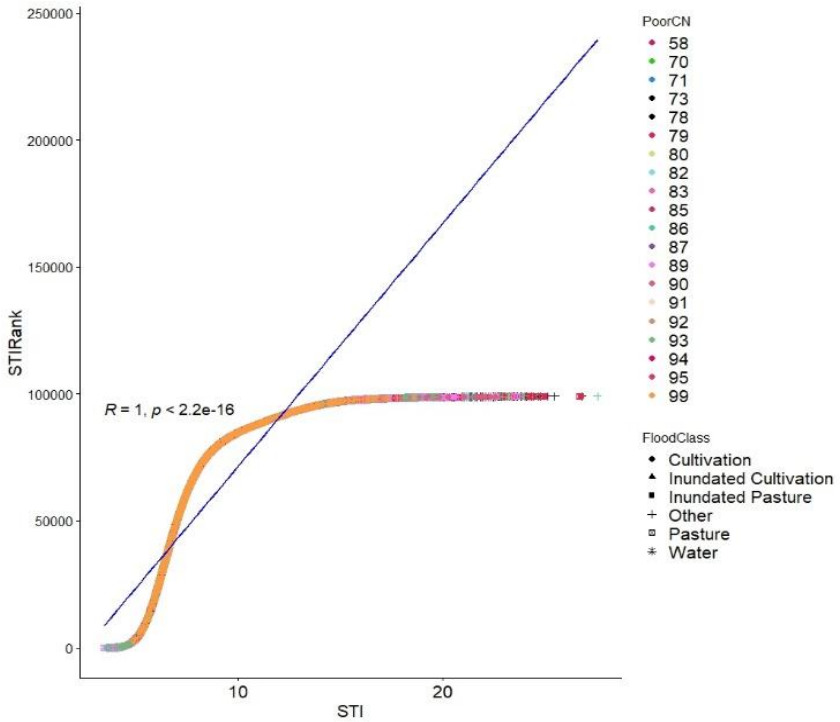

Figure 6a. STI values and Ranking of STI.

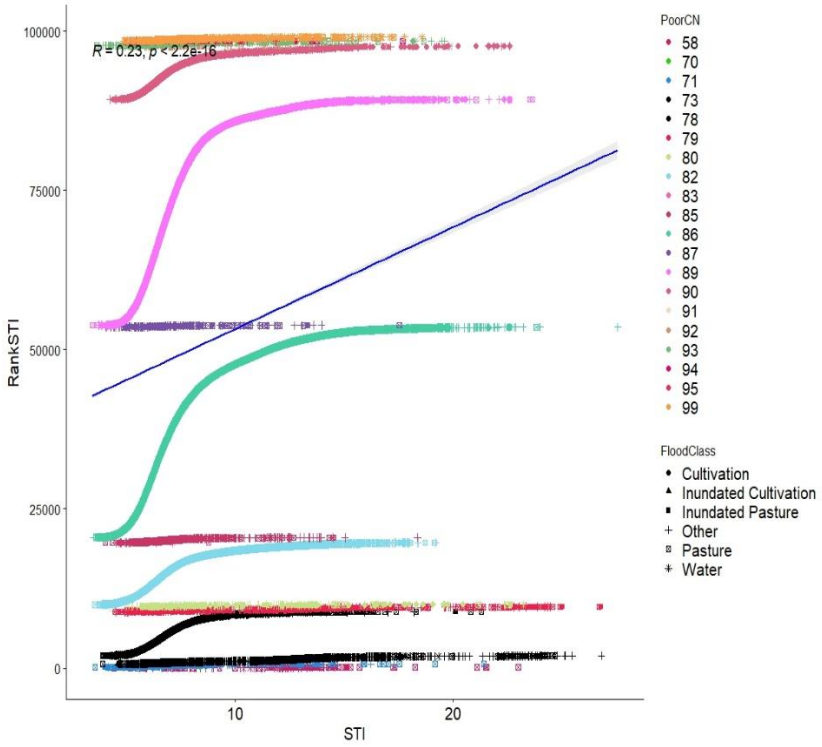

Figure 6b. STI values and Ranking based on Ranking of SCS–CN in poor and undrained condition.

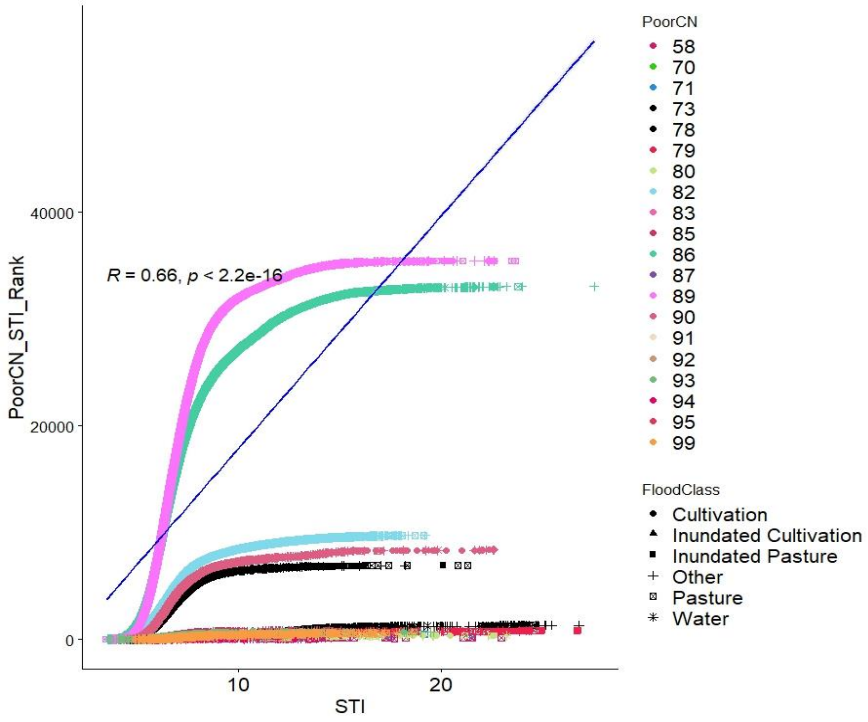

Figure 7. STI based on each CN values ranking map.

The ranking based on the increase of the STI ranking highly depends on the increase of SCS–CN values (Figure 6b). The idea is the ranking of STI depends on the increase of SCS–CN values rather than the increase of STI. Thus, correlation coefficient between STI values and ranking of STI was 0.28. First, SCS–CN values were increased from 58 to 99. Then The STI were sorted from smallest to largest. The lower SCS–CN values led to the lower ranking of STI. In the third ranking approach (Figure 7), STI ranking was based on each SCS–CN values ranking. First, SCS–CN values were arranged from smallest to largest. Second, in each

SCS–CN value, STI were arranged from 1 to largest. The correlation coefficient was 0.66 because the ranking depended on the increase of both SCS–CN values and STI values. In this case, ranking depend on STI values rather than SCS–CN values.

The Getis–Ord Gi* statistic computed a z–score in each feature in the dataset. For statistically significant positive z–scores, the larger the z–score is, the more intense the clustering of high values, named hot–spot. For statistically significant negative z–scores, the smaller the z–score is, the more intense the clustering of low values, named cold–spots. From three different ranking approaches, three different hot spot maps were generated, including a hot spot map of STI ranking, a hot spot map of STI based on SCS–CN values ranking, and a hot spot map of STI ranking based on STI in each SCS–CN values. Table 3 and figure 8 analyzed the distribution of hot spots and cold spots of the third ranking approach, in which STI ranking was arranged in each CN values, had the nearest distribution to the distribution of inundated areas in each LULC types.

Table 3. Total number of hotspots and cold spots in the third approach ranking map.

Hot spots and Cold spots in comparison with flooding map areas	**LULC types**	**Number of Cold spots**			**Number of Hot spots**			**Total cold spots and hot spots in each LULC types**
		–3	**–2**	**–1**	**1**	**2**	**3**	
Inundated Pasture	Corn						7	7
	Deciduous Forest	51	38	19	2			110
	Developed/Open Space		3		2	4		9
	Grass/Pasture	31	31	28	89	72	9	260
	Open Water				1	6	9	16
	Other Hay/Non–Alfalfa	52	37	4				93
	Soybeans				1	2	2	5
	Shrubland	3	1		1	1		6
Total cold spots and hot spots of inundated pasture in all LULC types		137	110	51	96	85	27	506
Inundated cultivation	Corn					2	30	32
	Deciduous Forest	4	2	1		1		8
	Developed/Open Space					2		2
	Grass/Pasture		1		2	7	3	13
	Open Water						1	1
	Other Hay/Non –Alfalfa	17	5	1				23
	Soybeans					1	8	9
Total cold spots and hot spots of inundated cultivation in all LULC types		21	8	2	2	12	34	88
Total cold spots and hot spots of inundated areas in all LULC types		158	118	53	98	97	61	594

Figure 8 illustrated the comparison between observed inundated areas and hot spot and cold spot distribution from the third approach ranking map. In table 3, total number of cold spots and hot spots in corn LULC areas in inundated cultivation and inundated pasture was 39 points, while the number in the observed inundated map was 40 points in corn LULC type (Figure 8). Generally, the number of hot spots and cold spots in the other LULC types declined in comparison to observed inundated areas. However, in three approaches of the ranking maps, the third ranking approach turned in the best result in comparison with observed inundated data.

Table 3 emerged distribution of hot spots and cold spots in each LULC type and compared to the distribution of inundated points in observed inundated areas. Accordingly, distribution in the hot spots map and inundated areas distribution in observed inundated areas had a similar tendency. The number of hot spots and cold spots decreased from corn to soybean. The highest number of hot spots and cold spots were in grass/pasture in both

distributions. However, the number of points were neither hot spots nor cold spots, which turned in 0 value from Getis–Ord Gi* spatial statistics, and were not analyzed in this description. Figure 9 illustrated the distribution of hot spots and cold spots of inundated cultivation added in google map of Callahan creek basin.

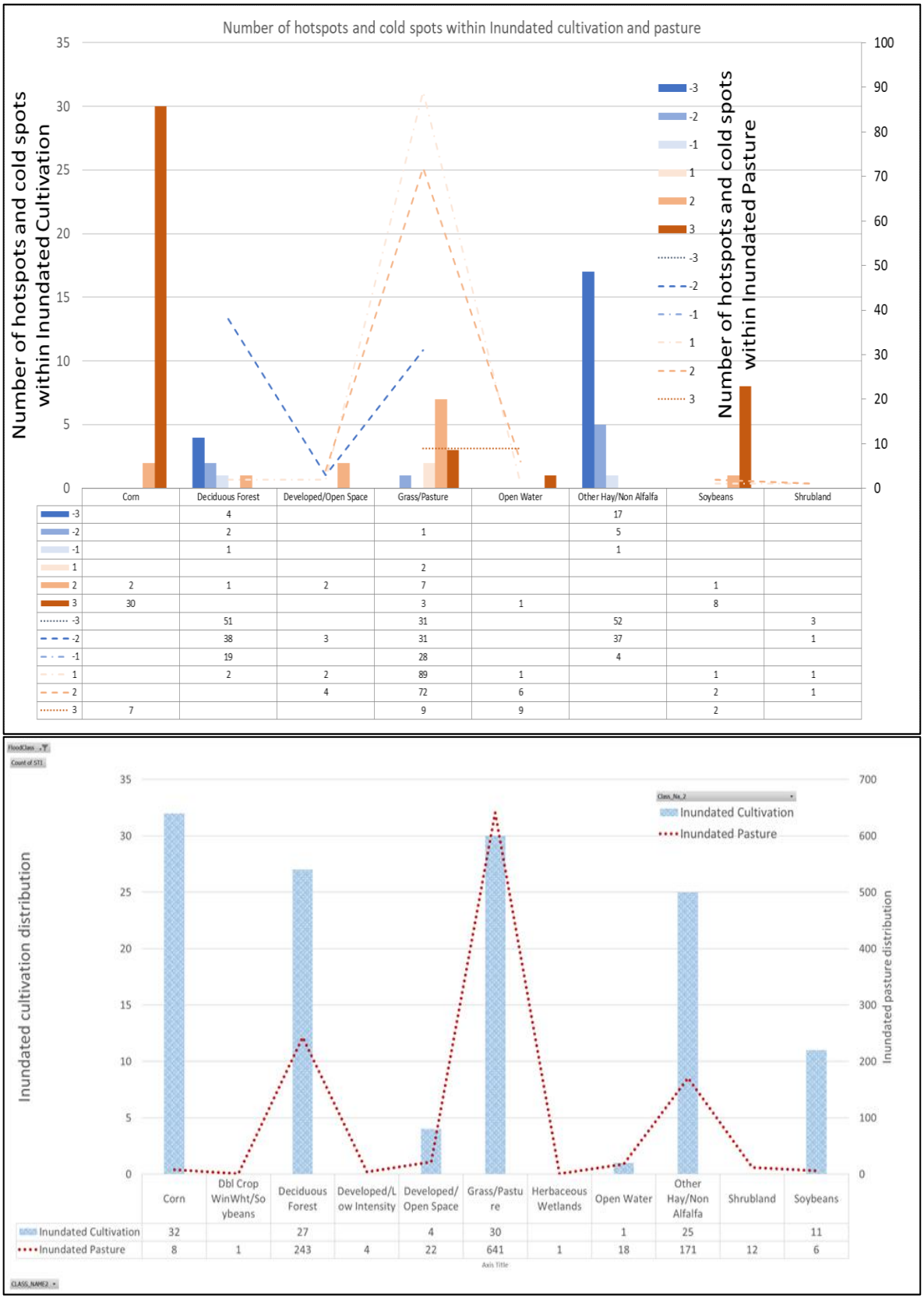

	Corn	Deciduous Forest	Developed/Open Space	Grass/Pasture	Open Water	Other Hay/Non Alfalfa	Soybeans	Shrubland
-3		4				17		
-2		2		1		5		
-1		1				1		
1				2				
2	2	1	2	7			1	
3	30			3	1		8	
-3		51		31		52		3
-2		38	3	31		37		1
-1		19		28		4		
1		2	2	89	1		1	1
2			4	72	6		2	1
3	7			9	9		2	

	Corn	Dbl Crop WinWht/Soybeans	Deciduous Forest	Developed/Low Intensity	Developed/Open Space	Grass/Pasture	Herbaceous Wetlands	Open Water	Other Hay/Non Alfalfa	Shrubland	Soybeans
Inundated Cultivation	32		27		4	30		1	25		11
Inundated Pasture	8	1	243	4	22	641	1	18	171	12	6

Figure 8. Comparison between observed inundated areas and hot spot and cold spot distribution from the third approach ranking map.

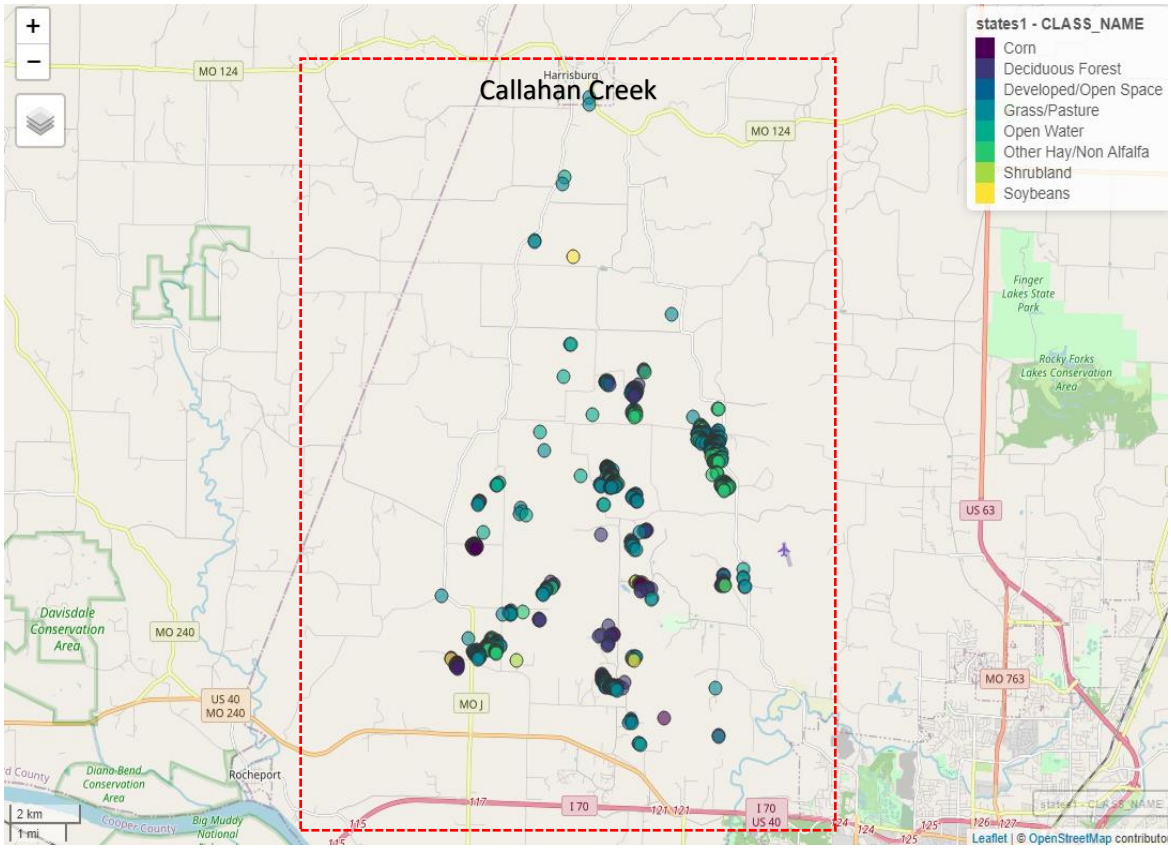

Figure 9. Distribution of hot spots and cold spots of inundated cultivation on google earth map.

4. Conclusions

There was a statistical significance of the greater STI in inundated cultivation than STI in cultivation areas. However, STI values were not significant in STI comparisons of pasture areas. This result requires further observation to analyze the complexity of hydrology in the study areas. In other words, saturated excess mechanism is insufficient to explain runoff generation in pasture areas in this watershed. Therefore, the combination between STI and SCS–CN values demonstrated by the statistical significance of inundated pasture STI refined the explanation of runoff generation mechanisms. At some SCS–CN value, STI in inundated pasture is statistically higher than those of drained pasture. Thus, strongly recommend that STI and SCS–CN values should be combined to produce a ranking map of high runoff potential areas. However, the results need to be validated by soil moisture monitoring or by field studies.

Hot spots and cold spots of runoff generation can emerge either within inundated areas or out of inundated areas. This challenge demands an appropriate scale analysis and hot spot generation mechanism since spatial and temporal resolutions of input data highly affect the hot spots of runoff generations. The distributions of hot spot and cold spots varied in each LULC type. This fluctuation requires high accuracy of land use land cover data as well as distribution of inundated areas. Ranking maps can be highly uncertain in many different runoff generation mechanisms. Therefore, it is necessary to be validated based on field research.

The saturated hydraulic conductivity values should be as precise as possible so that the values can represent the variation of spatial and temporal scale to emerge the hot spots and cold spots. Wilcoxon rank sum test highly depends on the rank sum value of observed data, and thus in this study, the quality of LULC data and observed inundated map significantly influences the results.

Author contribution statement: Data sources from USGS, USDA: seek and opt by Anh Bui KV; STI calculation following Soil and Water Lab document, Biological and Environmental Engineering, Cornell University. SCS–CN following USDA. Validation, Visualization: Application of GIS tools and R software. Literature review, methodology, research design, conducting calculation, data analysis, writing–original draft, writing–review & editing: Anh Bui KV.

Acknowledgements: The idea of hot spots in this study had been initially acquired at the University of Missouri, which was as a part of the research credits for research proposal in the Graduate Program at the School of Natural Resources, the University of Missouri. The ideology of SCS–CN and STI combination was initially mentioned in the research proposal in March 2019 – With gratitude for the support in research materials, insightful coursework and opportunities.

Conflicts of Interest: The author declares that there is no conflict of interest.

References

1. Walter, M.F.; Steenhuis, T.S.; Haith, D.A. Nonpoint Source Pollution Control by Soil and Water Conservation Practices. *Trans. Am. Soc. Agric. Eng.* **1979**, *22(4)*, 0834–0840.
2. Schneiderman, E.M. et al. Incorporating variable source area hydrology into a curve–number–based watershed model. *Hydrol. Process.* **2007**, *21*, 25, 3420–3430. doi: 10.1002/hyp.6556.
3. Tomer, M.D.; Dosskey, M.G.; Burkart, M.R.; James, D.E.; Helmers, M.J.; Eisenhauer, D.E. Methods to prioritize placement of riparian buffers for improved water quality. *Agrofor. Syst.* **2009**, *75(1)*, 17–25. doi: 10.1007/s10457-008-9134-5.
4. Delgado, J.; Gantzer, C.; Sassenrath, G. Soil and water conservation A celebration of 75 years. 2020.
5. Agnew, L.J. et al. Identifying hydrologically sensitive areas: Bridging the gap between science and application. *J. Environ. Manage.* **2006**, *78(1)*, 63–76. doi: 10.1016/j.jenvman.2005.04.021.
6. Buchanan, B. et al. Estimating dominant runoff modes across the conterminous United States. *Hydrol. Process.* **2018**, *32(26)*, 3881–3890. doi: 10.1002/hyp.13296.
7. Easton, Z.M.; Fuka, D.R.; Walter, M.T.; Cowan, D.M.; Schneiderman, E.M.; Steenhuis, T.S. Re–conceptualizing the soil and water assessment tool (SWAT) model to predict runoff from variable source areas. *J. Hydrol.* **2008**, *348(3–4)*, 279–291. doi: 10.1016/j.jhydrol.2007.10.008.
8. Lyon, S.W.; Walter, T.M.; Gerard–Marchant, P.; Steenhuis, T.S. Using a topographic index to distribute variable source area runoff predicted with the SCS curve–number equation. *Hydrol. Process.* **2004**, *18(15)*, 2757–2771. doi: 10.1002/hyp.1494.
9. Todd Walter, M.; Steenhuis, T.S.; Mehta, V.K.; Thongs, D.; Zion, M.; Schneiderman, E. Refined conceptualization of TOPMODEL for shallow subsurface flows. *Hydrol. Process.* **2002**, *16(10)*, 2041–2046. doi: 10.1002/hyp.5030.
10. Walter, M.T.; Walter, M.F.; Brooks, E.S.; Steenhuis, T.S.; Boll, J.; Weiler, K. Hydrologically sensitive areas: Variable source area hydrology implications for water quality risk assessment. *J. Soil Water Conserv.* **2000**, *55(3)*, 277–284.
11. Garen, D.C.; Moore, D.S. Curve Number (CN) hydrology in Water Quality Modeling. *JAWRA J. Am. Water Resour. Assoc.* **2005**, *3224(03127)*, 377–388.
12. McClain, M.E. et al. Biogeochemical Hot Spots and Hot Moments at the Interface of Terrestrial and Aquatic Ecosystems. *Ecosystems* **2003**, *6(4)*, 301–312. doi: 10.1007/s10021-003-0161-9.
13. USDA Conservation Engineering Division and NRCS. Urban Hydrology for Small.

Soil Conserv. No. Technical Release 55 (TR–55), 1986, pp. 164.
14. Zhan, X.; Huang, M.L. ArcCN–Runoff: An ArcGIS tool for generating curve number and runoff maps. *Environ. Model. Softw.* **2004**, *19(10)*, 875–879. doi: 10.1016/j.envsoft.2004.03.001.
15. Beven, K.J.; Kirkby, M.J. A physically based, variable contributing area model of basin hydrology. *Hydrol. Sci. Bull.* **1979**, *24(1)*, 43–69. doi: 10.1080/02626667909491834.
16. Dosskey, M.G.; Qiu, Z.; Helmers, M.J.; Eisenhauer, D.E. Improved indexes for targeting placement of buffers of Hortonian runoff. *J. Soil Water Conserv.* **2011**, *66(6)*, 362–372. doi:10.2489/jswc.66.6.362.
17. Buchanan, B.P. et al. Evaluating topographic wetness indices across central New York agricultural landscapes. *Hydrol. Earth Syst. Sci.* **2014**, *18(8)*, 3279–3299. doi: 10.5194/hess-18-3279-2014.
18. Qiu, Z.; Lyon, S.W.; Creveling, E. Defining a Topographic Index Threshold to Delineate Hydrologically Sensitive Areas for Water Resources Planning and Management. *Water Resour. Manag.* **2020**, *34*, 3675–3688. doi:10.1007/s11269-020-02643-z.
19. Anselin, L. Local Indicators of Spatial Association–LISA. *Geogr. Anal.* **1995**, *27(2)*, 93–115. doi: 10.1111/j.1538-4632.1995.tb00338.x.
20. Getis, A.; Ord, J.K. The Analysis of Spatial Association by Use of Distance Statistics. *Geogr. Anal.* **1992**, *24(3)*, 189–206. doi: 10.1111/j.1538-4632.1992.tb00261.x.
21. Ord, J.K.; Getis, A. Local Spatial Autocorrelation Statistics: Distributional Issues and an Application. *Geogr. Anal.* **1995**, *27(4)*, 286–306. doi:10.1111/j.1538-4632.1995.tb00912.x.
22. Tobler, W. On the first law of geography: A reply. *Ann. Assoc. Am. Geogr.* **2004**, *94(2)*, 304–310. doi:10.1111/j.1467-8306.2004.09402009.x.